

Advancing InGaN VCSELs

Mike Cooke reports on progress towards filling the green gap and improving tunnel junctions as alternatives to indium tin oxide current-spreading layers.

Vertical-cavity surface-emitting lasers (VCSELs) promise advantages over the more traditional edge-emitting lasers, such as the potential for reduced manufacturing costs, integrated electronics, parallel array structures, and lower input power operation. VCSELs have been produced for a long time using aluminium gallium arsenide (AlGaAs) technology, but such devices are restricted to red-infrared wavelengths longer than 650nm. For shorter wavelengths one naturally looks to III-nitride (III-N) materials, where the III stands for metals such as gallium (Ga), indium (In) and aluminium (Al).

However, there are many difficulties in developing VCSELs, particularly for the longer green-yellow-orange wavelengths that would extend the reach of the red devices. The problems are the often cited ones for III-N light emitters in general: lattice mismatches leading to defects; different charge polarizations of the various ionic bonds between the group III metals and nitrogen, creating electric fields that inhibit electron-hole recombination into photons; difficulties

of incorporating indium for the longer wavelengths, and so on.

VCSELs offer desirable characteristics such as compactness, low thresholds, large modulation bandwidth, narrow linewidths, and circular beam patterns. Along with 'green gap' filling, moving to shorter ultraviolet wavelengths could challenge bulky gas and solid-state lasers such as 325nm helium-cadmium lasers, 355nm neodymium-doped yttrium aluminium garnet (Nd:YAG) lasers, and excimer lasers for applications.

Possible uses could be for high-resolution laser printers, laser lighting, visible light communication (free-space and plastic fiber) and bio-sensing

Other possible uses could be for high-resolution laser printers, laser lighting, visible light communication (free-space and plastic fiber) and bio-sensing.

Near-green lasing

Xiamen University and Suzhou Institute of Nano-Tech and Nano-Bionics

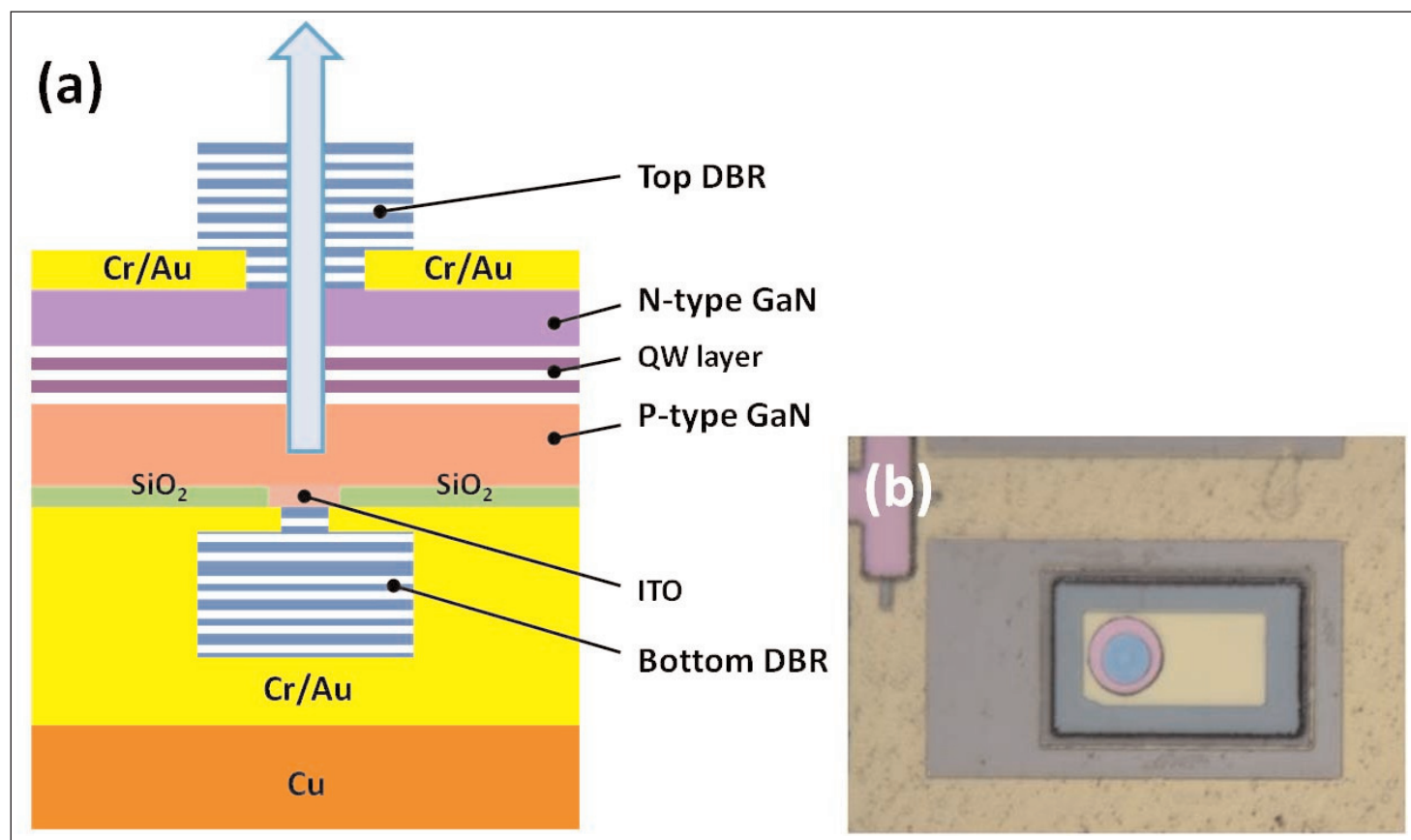


Figure 1. (a) Cross-sectional schematic of VCSEL. (b) Optical image of real device.

(SINANO) in China have developed near-green VCSELS using material that is mainly luminescent in the blue 445nm part of the spectrum [Rongbin Xu et al, IEEE Transactions on Electron Devices, vol 65, issue 10 (October 2018), p4401].

The researchers engineered the cavity resonance so that it favored the near-green 493nm-wavelength emissions from InGaN. Efficient green laser diodes are highly desired to plug the 'green gap' for red-green-blue full-color display systems. Presently, green laser light is produced using a combination of a longer-wavelength lasers and frequency-doubling materials, increasing complexity, system sizes, and cost.

The active region consisted of a double quantum well of $\text{In}_{0.18}\text{Ga}_{0.82}\text{N}$, of 2.5nm each, separated by 6nm of GaN. Normally, such material is expected to emit blue wavelengths around 445nm. The wells were capped with an electron-blocking layer of 20nm $\text{Al}_{0.2}\text{Ga}_{0.8}\text{N}$ to prevent carrier overflow into the p-type layers. The metal-organic chemical vapor deposition (MOCVD) of III-nitride material was performed on c-plane sapphire.

The epitaxial material was fabricated into a VCSEL (Figure 1) with distributed Bragg reflector (DBR) mirrors defining the cavity and silicon dioxide (SiO_2) defining the current aperture. The DBRs used titanium oxide (Ti_2O_3) and SiO_2 dielectric pairs — 13.5 for the bottom mirror and 11.5 for the top. Indium tin oxide (ITO, 30nm) was used for current spreading in the aperture. The p- and n-electrodes were both chromium/gold (Cr/Au). The structure was flipped onto a copper (Cu) heatsink.

At low 15mA current, the emission centers on the ~440nm blue range of the InGaN quantum well material (Figure 2). As the current increases to the 32mA (~18kA/cm²) threshold, the wavelengths in the cavity resonance region of 493nm become stronger, based on emissions from indium-rich localized narrow-bandgap regions. At higher 45mA current injection, the ~440nm wavelengths are suppressed and a narrow lasing peak emerges with 0.55nm linewidth in the blue-green 493nm region. The output power at 50mA was estimated to be ~178μW.

Previously, researchers from Xiamen, along with East China Normal University, SINANO, Technical University of Berlin in Germany and Taiwan Chiao Tung University reported quantum dot VCSELS in the green region (491.8–565.7nm), but with only ~10μW light output power [Yang Mei et al, Light: Science & Applications, vol6, pe16199, 2017]. At the time, the longest wavelength of 565.7nm and threshold currents as low as 0.52mA (0.66kA/cm²) constituted records for green VCSELS. The devices also depended on the effect of cavity length on the lasing wavelength.

The optical polarization of the emitted light from the more recent quantum well VCSEL was 71% at 1.09x the threshold current injection.

The cavity resonance compensates for the lower

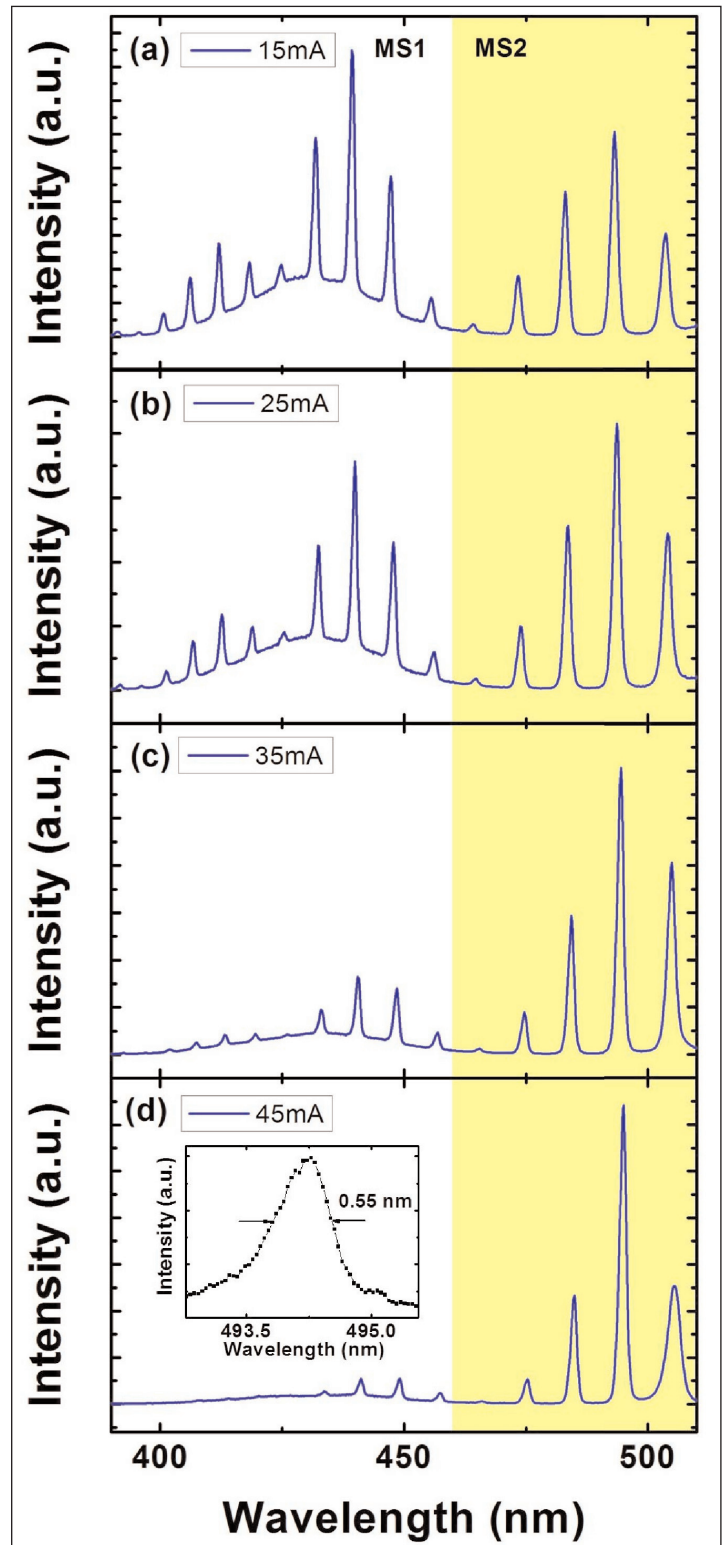


Figure 2. Electroluminescence spectra of the VCSEL measured at four different currents: (a) 15mA, (b) 25mA, (c) 35mA, and (d) 45mA. Inset: linewidth of lasing peak measured with higher resolution.

density of indium-rich localized narrow-gap regions, reducing the lifetime for recombination into photons. The researchers comment: "The short lifetime indicates a high carrier capture efficiency and can compensate the low density of emission centers, resulting in stronger emission intensity."

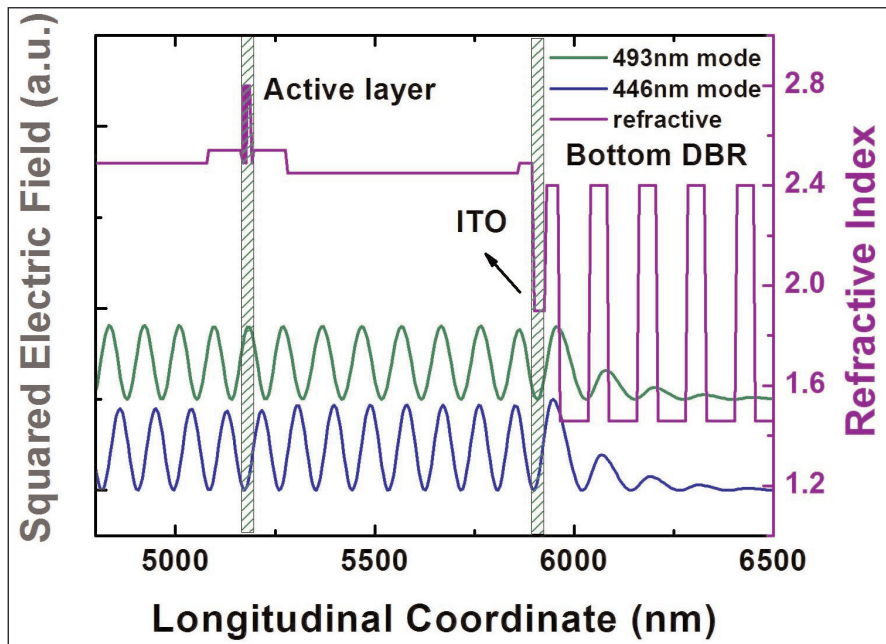


Figure 3. Refractive index and distribution of optical field for 446nm and 493nm cavity modes of VCSEL.

Simulations of the optical field also suggest that the active region lines up with an anti-node (maximum) of the standing-wave pattern for 493nm-wavelength emissions (Figure 3). By contrast, the 446nm mode gives a node (minimum) at the active layers. The gain enhancement factor is calculated at 1.82 for 493nm and 0.21 for 446nm. The researchers also point out that the longer lasing wavelength also benefits from less absorption loss in the active region.

Lowering thresholds

Xiamen also claims the lowest threshold energy density so far reported for an optically-pumped VCSEL based on InGaN technology [Jin-Zhao Wu et al, IEEE Transactions on Electron Devices, vol 65, issue 6 (June 2018), p2504]. The ultra-low 413µJ/cm² threshold was enabled by using a very short cavity, the knock-on effects of which included lower optical losses and higher gain. The team hopes its work will help guide III-nitride VCSEL improvements in the future.

MOCVD on sapphire created a laser structure with a multiple quantum well (MQW) active layer (Figure 4).

A 16.5-period Ti₃O₅/SiO₂ distributed Bragg reflector (DBR) was electron-beam evaporated before flipping the structure and bonding to a quartz substrate. This bottom DBR had a 99.9% reflectivity.

A lift-off process using 248nm excimer laser light removed the sapphire substrate. The cavity was then tuned to six wavelengths with “cautious” inductively coupled plasma etching and chemical mechanical polishing (CMP), giving a smooth surface with 0.1nm root-mean-square roughness. The structure was completed with 12.5-pairs of Ti₃O₅/SiO₂ for the top DBR. The MQW was placed at the antinode of the standing wave in the laser cavity to increase coupling with the gain medium (~1.7x enhancement).

The excitation consisted of 355nm-wavelength light from a Nd:YAG laser focused on a 50µm-diameter spot. The very short 6-wavelength cavity enabled a low laser threshold power density of 413µJ/cm² (8.12nJ/pulse, Figure 5). The wavelength was 415.9nm.

The researchers report that a previous 18-wavelength device had a 15x higher threshold of 6.3µJ/cm² (compared with 0.413mJ/cm² = 413mJ/cm², Figure 6). The researchers also estimate that the spontaneous emission factor increased by a factor of 7.7. They also calculate that the short-cavity gain was enhanced 3x and the round-trip optical absorption reduced 3x.

The polarization degree of the laser light was 91% at 2.2x threshold excitation.

Tunnel junctions

University of California Santa Barbara (UCSB) in the USA claims the first demonstration of a III-nitride semiconductor VCSEL with a tunnel junction (TJ) on the p-side using only MOCVD material growth [SeungGeun Lee et al, Appl. Phys. Express, vol11, p062703, 2018].

Tunnel junctions are seen as an alternative to indium tin oxide as a current-spreading material on the p-side of light-emitting III-nitride devices. Indium tin oxide

Gain medium	p-GaN	200nm	DBR	12.5x(Ti ₃ O ₅ /SiO ₂)
MQW	5x(In _{0.01} Ga _{0.99} N/In _{0.12} Ga _{0.88} N)	5x(4nm/4nm)	Gain	n-GaN
Gain medium	n-GaN	3µm	MQW	5x(In _{0.01} Ga _{0.99} N/In _{0.12} Ga _{0.88} N)
Buffer	GaN	2µm	Galn	p-GaN
Nucleation	Low-temperature GaN	30nm	DBR	16.5x(Ti ₃ O ₅ /SiO ₂)
Substrate	Sapphire		Substrate	Quartz

Figure 4. (left) Epitaxial structure; (right) VCSEL structure.

Figure 5. (a) Emission spectra dependence on pumping energy. (b) Emission intensity as a function of pumping energy. (c) Polarization characterization on pumping energy. (d) Spontaneous emission factor.

increases laser threshold currents and absorbs light, reducing efficiency.

Tunnel junctions of heavily doped p- and n-type material have been created before for VCSELs, but the UCSB team reports that these have used hybrid growth processes involving MOCVD and molecular beam epitaxy (MBE). An MOCVD-only process is preferred, since MBE is performed at lower temperatures, leading to higher defect density and impurity incorporation. Defects and impurities increase non-radiative recombination, reducing efficiency.

The VCSEL epitaxial material consisted of layers grown by MOCVD on bulk m-plane GaN, miscut -1° in the c-direction. Growth was carried out in two steps to allow activation of the buried p-type layers. Such layers suffer from hydrogen passivation, which hampers the acceptors from grabbing electrons to create holes in the valence band. An important aspect of activation is to drive out the hydrogen, usually with thermal annealing. Buried layers have less surface area — just the sidewalls — through which hydrogen can escape.

Between the initial growth and re-growth, the p^{++} -GaN was treated with buffered hydrofluoric acid (BHF) to remove excess magnesium, reducing diffusion into the subsequent n^{++} -GaN layer. When the wafer was returned to the MOCVD chamber, the temperature was held at 750°C for 5 minutes to activate in-situ the p-GaN material before MOCVD regrowth at 900°C .

The tunnel-junction structure was optimized with several experimental processes. A test structure with in-situ activation annealing had a 1.1V reduced forward voltage for a $1\text{kA}/\text{cm}^2$ current density. The performance of the in-situ activation was similar to a structure grown using a standard ex situ anneal at 600°C for 10 minutes in air (less than 0.1V difference over the test range).

The effect of the buffered hydrofluoric acid treatment was a 0.5V reduction of forward voltage at $1\text{kA}/\text{cm}^2$. "We believe that the BHF treatment improved the volt-

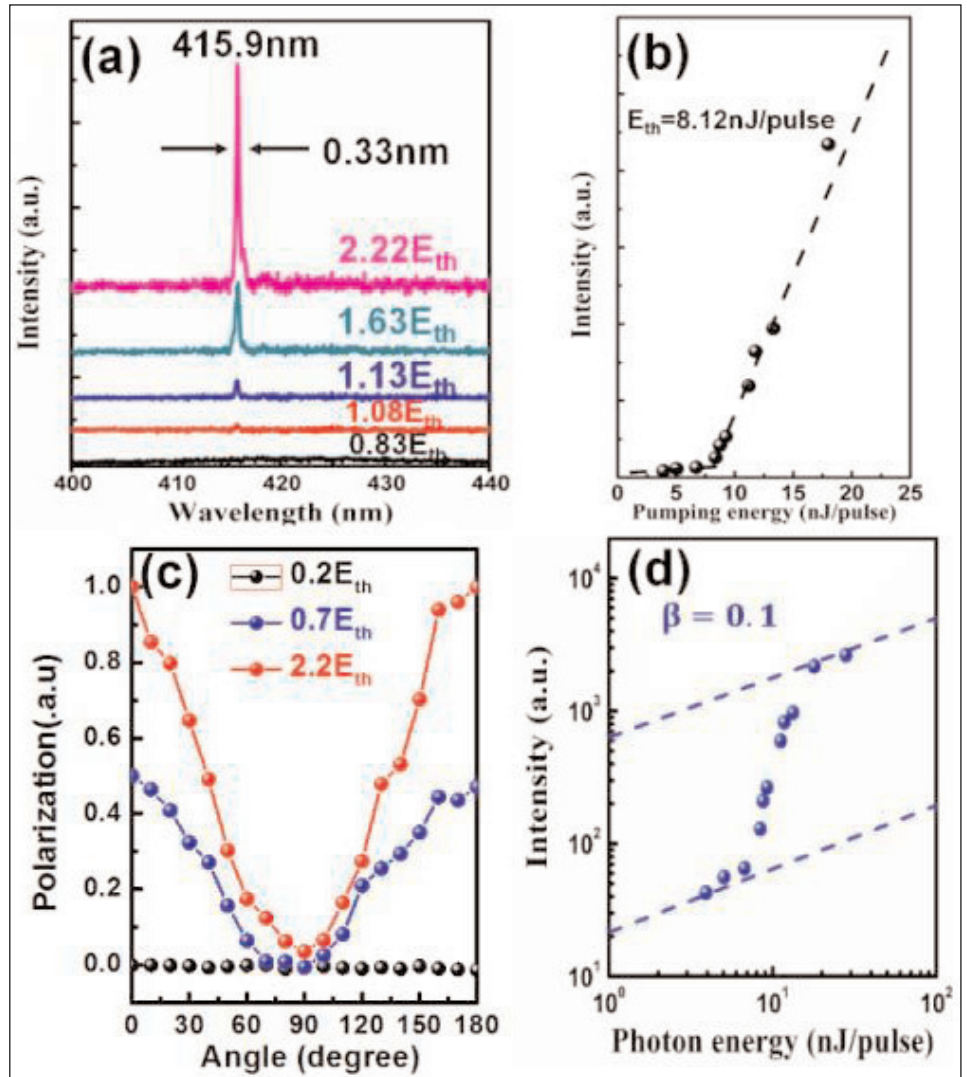
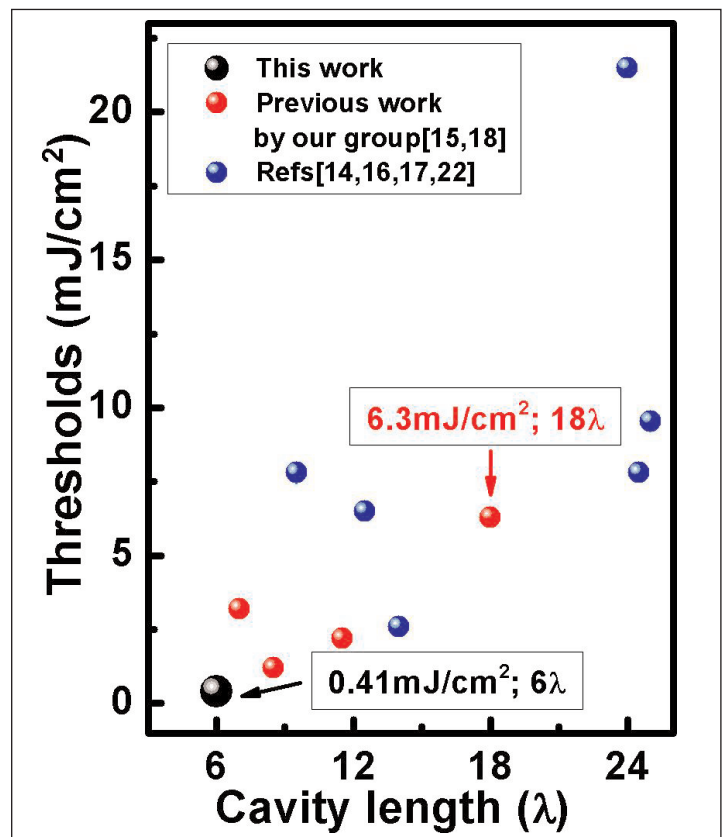


Figure 6. Statistics of thresholds of optical injection VCSEL.



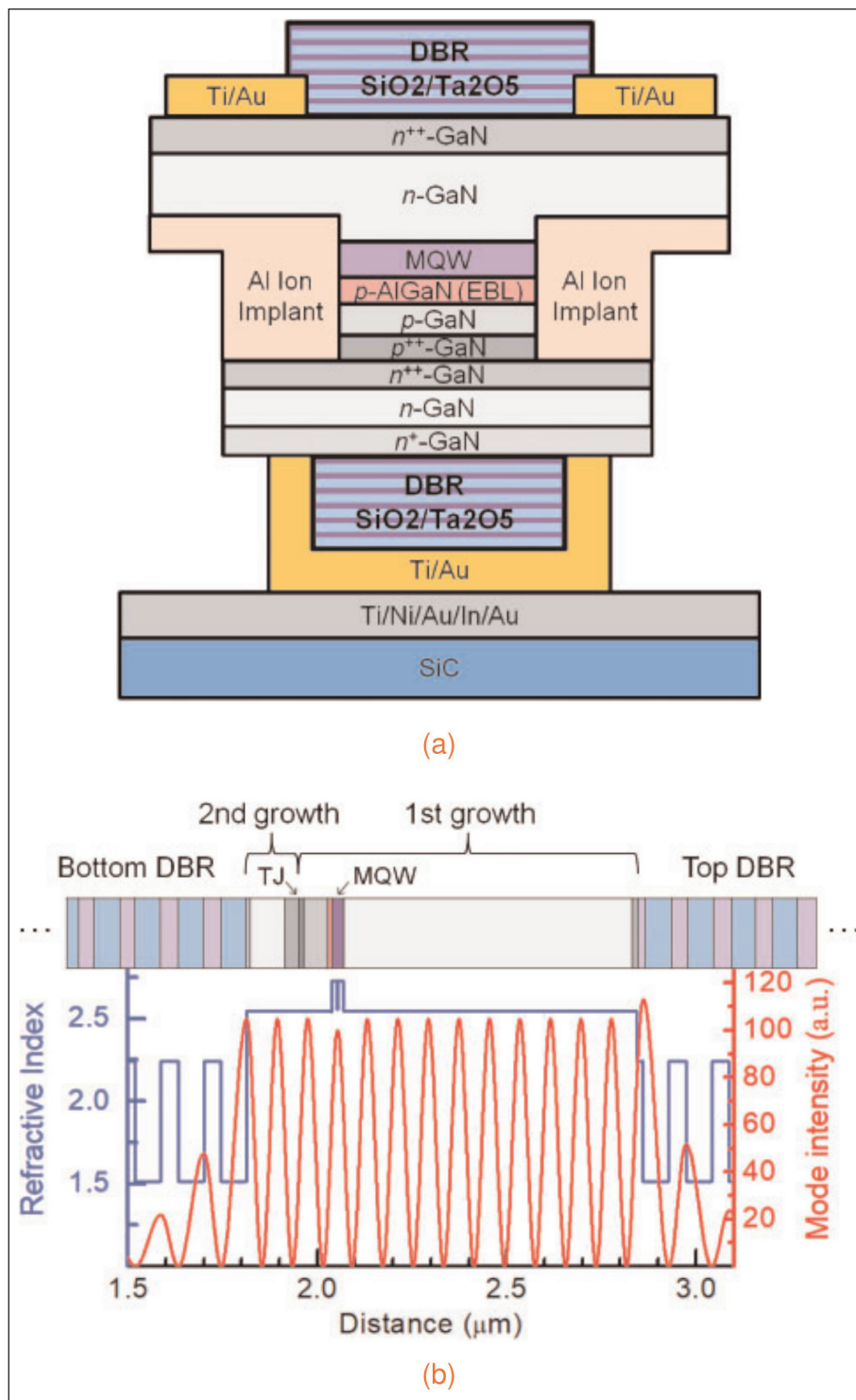


Figure 7. (a) Schematic of flip-chip VCSEL structure with dual dielectric DBRs and MOCVD-grown TJ contact and (b) cavity-mode intensity distribution overlaid with refractive index profile.

age by reducing Mg diffusion into the n⁺⁺-GaN layer, which could compensate electron carriers required to form an abrupt junction," the researchers comment.

Combining the BHF treatment with in-situ activation gave tunnel junctions with 3.4V forward voltage at 20A/cm² and 4.5V at 1kA/cm², close to the performance of junctions grown using a hybrid MOCVD/MBE process (3.05V at 20A/cm²) by a similar research team based at UCSB.

For the VCSEL (Figure 7, Table 1), the epitaxial structure was first grown to the p⁺⁺-GaN layer, followed by mesa etch and aluminium ion implantation to form the device aperture. Then the tunnel-junction growth was prepared with aqua regia and BHF treatments. After the tunnel-junction growth, a 17-period DBR consisting of SiO₂ and tantalum pentoxide (Ta₂O₅) layers was deposited, followed by titanium/gold (Ti/Au) contact metals.

The device structure was then flipped and bonded onto metal layers consisting of titanium/nickel/gold/indium/gold (Ti/Ni/Au/In/Au) on a silicon carbide substrate. The GaN growth substrate was removed by photo-electro-chemical (PEC) etching of a sacrificial MQW. The VCSEL was completed with deposition of Ti/Au contact metals and a 13-period DBR. The n⁺⁺-GaN and DBR were separated by a 1/8-wavelength layer of Ta₂O₅.

The VCSEL was characterized using pulsed operation, presumably to avoid self-heating effects. The threshold for lasing occurred at 10kA/cm² current density (15mA current) and 7.8V forward bias. The maximum output power was 319μW with 55kA/cm² injection and 12V bias. Kinks in the output power behavior were likely due to higher orders contributing to the lasing. The wavelength was 408nm with ~1.9nm full-width at half maximum (FWHM) at 20mA injection. The accuracy of the linewidth was limited by the spectrometer's resolution capability.

The differential efficiency reached 0.28%. The differential resistivity of the tunnel junction was 10⁻⁴Ω-cm², higher than the 5x10⁻⁵Ω-cm² for the previously reported tunnel junction from a hybrid growth process. "We believe that the low doping concentrations of the current-spreading layers on the p-side are the main cause of the high differential resistivity that limits the device performance", the

researchers comment.

Optical microscope inspection of the 14μm-diameter aperture during lasing showed lasing spots that increased in number as the injection current increased (Figure 8). Some of the lasing filaments were at the original frequency; others contributed higher modes. The non-uniformity is attributed by the team to poor current spreading and variations of the tunnel-junction contact resistance. The researchers also suggest that

Table 1. VCSEL epitaxial layer structure grown on m-plane GaN substrate. (UID: unintentionally doped.)

Epitaxial layer	Thickness	Doping concentration	Contribution to internal optical loss
2nd growth			
n ⁺ -GaN	10nm	10 ¹⁹ /cm ³	1.8%
n-GaN	94nm	1.3x10 ¹⁸ /cm ³	6.0%
n ⁺⁺ -GaN	40nm	10 ²⁰ /cm ³	9.4%
1st growth			
p ⁺⁺ -GaN	14nm	2.2x10 ²⁰ /cm ³	21.7%
p-GaN	61.2nm	10 ¹⁹ /cm ³	12.8%
p-AlGaN	5nm	2.2x10 ¹⁹ /cm ³	1.3%
2x(InGaN/GaN) MQW	2x(1nm/14nm)	UID	
n-GaN	759.4nm	2.3x10 ¹⁸ /cm ³	45.7%
n ⁺ -GaN	15nm	1.7x10 ¹⁹ /cm ³	1.3%
InGaN (sacrificial QW)	7nm	UID	
n-GaN (template)	~1300nm	1.3x10 ¹⁸ /cm ³	

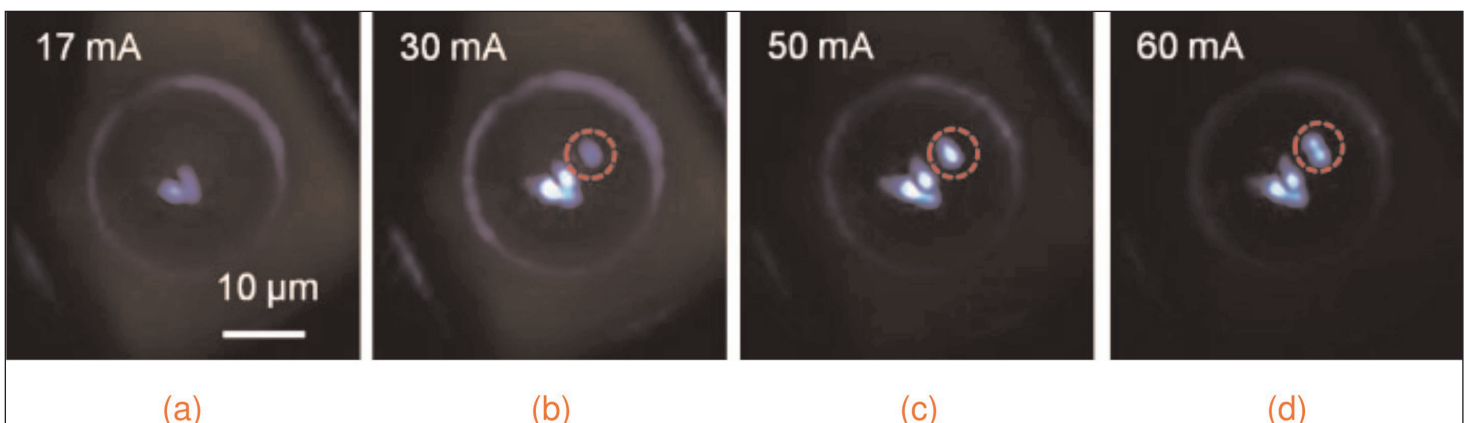


Figure 8. Optical microscopy images of VCSEL as a function of current above threshold (~15mA). Exposure times of the camera were the same for (a) and (b) and reduced for (c) and (d) to obtain clear images. Lasing spots in red circles show switching to higher-order mode.

surface residues such as gallium oxide left after the GaN substrate removal could play a role in the non-uniformity. ■

Author: Mike Cooke is a freelance technology journalist who has worked in the semiconductor and advanced technology sectors since 1997.

REGISTER
for *Semiconductor Today*
free at
www.semiconductor-today.com